J. Biochem. **136**, 457–462 (2004)
DOI: 10.1093/jb/mvh156

Cytotoxic and Membrane Perturbation Effects of a Novel Amyloid Forming Model Peptide Poly(Leucine-Glutamic Acid)

Rajadas Jayakumar*, Jayaraman Murali, Deenadayalan Koteeswari and Kannayiram Gomathi

Bio-organic and Neurochemistry Division, Central Leather Research Institute, Adyar, Chennai, 600 020, India

Received May 18, 2004; Accepted July 8, 2004

In the present study we have elucidated the toxicity of a novel amyloid forming model peptide, Poly (leucine-glutamic acid). The toxicity of the fibrils prepared from this peptide was analyzed in peripheral blood lymphocytes (PBL). The MTT reduction assay revealed that the viability of PBL decreases significantly upon treatment with Poly(leucine-glutamic acid) (Poly [LE]). Enhanced DCFH-DA fluorescence in treated cells suggests that peptide toxicity is probably mediated by the formation of free radicals. *In vivo* and *in vitro* biochemical studies indicated that Poly [LE] inactivates the antioxidant system of cells. Perturbation of Poly [LE] in a membrane lipid environment was assessed by circular dichroism (CD) using phosphotidyl choline-cholesterol bilayers. The CD results revealed that LE enhances its beta sheet content in a bilayer environment. Sequestration of Poly [LE] in lipid rafts demonstrates that it has a binding cleft similar to Aβ in lymphocyte raft domains. Nuclear membrane binding studies showed that Poly [LE] binds to nuclear membranes and may cause genotoxicity.

Key words: β amyloid, cytotoxicity, lipid raft, nuclear membrane, poly(leucine-glutamic acid).

Huntington's, Alzheimer's and prion diseases of degenerative disorders of the brain (*1*). Although their etiology and pathogenesis are not fully understood, increasing evidence points to abnormal amyloid fibril formation as a general mechanism behind a diverse group of these neurodegenerative diseases (*2*). Amyloid is composed of misfolded beta sheet rich proteins that assemble spontaneously into protofibrils, and then form higher order structures ranging from simple twisted pairs of helical fibrils to insoluble quaternary structures with extensive beta sheet content. Although different cellular proteins misfold in different diseases, fibrils share a common structure that confers distinctive biochemical properties shared by all other amyloid deposits (*3*). These properties include diagnostic green birefringence in the presence of CongoRed, attributable to the characteristic cross beta structure of the fibrils (*4*). Several studies have shown that the extent of beta sheet formation is directly correlated with the ability to form amyloid fibrils (*5*). A significant problem in studying these structures and their self-organization into fibrillar structures is the poor solubility of the intermolecularly associated beta strands (*6*). To broaden the understanding of beta sheet formation, stabilization and associated aggregation, well-defined soluble peptide models are needed. Designing peptide-based molecules to adopt beta sheet folding and a fibrillar structure similar to amyloid fibrils has provided useful information for constructing and manipulating peptide conformation and elucidating complex folding mechanisms. To evaluate the proposed formation of beta sheet in amyloidic peptides, we designed a model peptide comprising alternating bulky hydrophobic (leucine) and hydrophilic (glutamic acid) residues. We have recently reported that an admixture of random coil with turns of monomeric poly [LE] undergoes a conformational transition into beta sheet by forming fibrils and exhibiting structural similarities to naturally occurring amyloid fibrils (*7*). Similarities in the physical properties of Poly [LE] and other known amyloids led us to study its mechanism of toxicity. To evaluate toxicity in a biological system, we used normal human lymphocytes.

The rationale for selecting lymphocytes is based on the fact that they have been demonstrated to be a cell model in which to study oxidative stress and DNA damage in neurodegenerative diseases (*8*). Thus lymphocytes represent a remarkable example of a non-neuronal model that can provide insight into the biological response to amyloidic oxidative stress stimuli by displaying different cell death pathways (*9*). The main objective of this study was to evaluate the crucial role of Poly [LE] in the cytotoxicity on lymphocytes. Poly [LE] induced radicals were determined by 2,7 dichlorofluorescein diacetate, fluorescence and associated changes in the antioxidant system were evaluated by biochemical parameters. Cytotoxicity was estimated by MTT, and a comet assay was used to study DNA damage. The perturbation of amyloid in membranes was carried out in lipid rafts and nuclear membranes to assess the mode of interaction of Poly (LE) with membranes.

MATERIALS AND METHODS

Synthesis of Poly (Leu-Glu)—Poly [LE] was synthesized by the condensation of the corresponding dipeptide-*O*-phenolic esters by a conventional solution phase method

*To whom correspondence should be addressed. Phone: +91-44-24911386 (Ext. 324), Fax: +91-44-24911589, E-mail: karkuvi77@hotmail.com

using the DCC technique. The *O*-benzyl oxy phenyl ester of γ-benzyl-L-glutamate (5 mM) was neutralized with triethylamine, and the free amine was extracted with ethylacetate. After the solvent was evaporated, the ester was taken up in DMF, and then Boc-Leu (5 mM) and DCC (5.5 mM) were added. The mixture was stirred for 4 h at 5°C and then left overnight. DCU was filtered and the filtrate was evaporated. The dipeptide ester was taken up in DMF and polymerization was initiated by increasing the pH to 9 using the initiator TEA. After stirring for 5–6 h, the unreacted monomer was washed with ethyl acetate, and the crude polymer was lyophilized. The lyophilized peptide was purified by HPLC and characterized by FTIR and CD, and stored at 4°C. The molecular weight was determined by gel permeation chromatography and found to be 35000 (~51 dipeptide repeats).

Amyloid Fibril Preparation—Fibril formation was initiated by incubating the polypeptide dissolved in phosphate buffer at 37°C (1 mg/ml). Fibril growth was monitored by thioflavin-T fluorescence until complete. The change in secondary conformation during fibril formation was determined by CD spectroscopy. The quality of fibrils was assessed by electron microscopy as described in our previous work (*7*). Sulfo NHS- Biotin (Pierce Biotech, Rockford, Il) was used to biotinylate LE.

Isolation of peripheral blood lymphocytes (PBL): Heparinized blood obtained from normal healthy volunteers was layered over lymphoprep gradient (Sigma Chemicals St. Louis., MO) and centrifuged at 1,880 rpm for 40 min, after which the top-two thirds of the supernatant was removed. The PBL were aspirated and washed twice with RPMI-1640 medium (Sigma). Cell viability was determined by the trypan blue exclusion test.

Peptide toxicity studies: PBLs were plated in 96-well Microtiter plates (Tarson) at a cell density of 2×10^5 cells/well. The PBLs were suspended in serum-starved medium, RPMI-1640, containing L-glutamine (2 M) and gentamycin (80 mg/liter). The cells were incubated with poly (LE) fibril, at a concentration of 1.5, 2.5, 5, 7.5 and 10 μM/ml and $A\beta b_{25–35}$ fibrils at a concentration of 5 μM/ml. All incubations were performed in triplicate. Cells without peptides were considered controls and incubated at 37°C in a 5% CO_2 incubator for 3 days. Aliquots of incubated cells were removed and washed with PBS and used for analysis.

MTT reduction assay: Treated PBLs were assessed by the MTT reduction assay as previously described (*10*). MTT reduction was measured on a micro-ELISA reader at a test wavelength of 570 nm and reference wavelength of 630 nm.

Biochemical parameters: PBLs were incubated with poly (LE) fibrils and $A\beta_{25–35}$ fibrils at a concentration of 5 μM/ml, incubations were performed in triplicate. Lipid peroxidation was determined by the method of Ohkawa *et al.* (*11*). GSH was measured using the method of Moron *et al.* (*12*).Superoxidedismutase was assayed using method of Misra and Fridovich (*13*). Total ATPases was assayed using method of Evans (*14*).

Interaction of superoxide dismutase with amyloids: Superoxide dismutase was purchased from (Sigma) and used directly for experiments. Superoxide dismutase (200 units/ml) was incubated at different temperatures (as given in figure legends) with 5 μM of amyloid, and the activities of incubated enzymes were analysed by a standard protocol (*13*).

Genotoxicity studies—Comet assay: DNA damage was detected by the comet assay according to the method described earlier (*15*). Briefly, fully frosted slides were covered with 0.7% normal-heating agarose as the first layer, Amyloid -treated cells were harvested and washed with PBS, and mixed with 0.7%low melting agarose as the second layer. The third layer comprised 0.7% low melting agarose. After solidification at 4°C, the slides were immersed in lysing buffer at 4°C for 1 h, and then placed in an electrophoresis tank filled with freshly prepared electrophoresis solution for 20 min. The slides were then neutralized in neutralization buffer, stained with ethidium bromide, and examined under a fluorescence microscope (Nikon).

Assessment of free radicals in lymphocytes (16): The levels of radicals generated in lymphocytes were measured using DCFH-DA (Sigma) as a fluorescence probe. The principle of this assay is that DCFH-DA diffuses through the cell membrane and is enzymatically hydrolyzed by intracellular esterases to nonfluorescent DCFH. In the presence of reactive oxygen species (ROS) this compound is rapidly oxidized to highly fluorescent dichlorofluorescein (DCF). A stock solution of 5 mM DCFH-DA in absolute ethanol was prepared and kept at in the dark. Cells were incubated for 4 h with DCFH-DA and assayed spectrofluorimetrically at an excitation wavelength of 488 nm and emission wavelength of 530 nm.

Peptide-membrane interaction—Isolation of lipid rafts from lymphocytes: PBLs were incubated with 5 μm of biotinylated poly LE and $A\beta_{25–35,}$ harvested, washed in phosphate buffered saline, pH 7.4, and then incubated with FITC- Streptavdin (SRL, India). The cells were then washed and incubated with Triton X 100 for 10 min at 4°C. The lysed cells were layered over sucrose gradient (10, 20, and 30%), and centrifuged at $2,500 \times g$ for 50 min. The layer containing detergent resistant membrane (DRM) fragment was carefully removed and analysed for amyloid binding on raft and non-raft regions (*17*).

Isolation of nuclear membrane from lymphocytes (18): Biotinylated peptide–treated PBL were harvested and washed in phosphate buffered saline, pH 7.4, and then, incubated with FITC-Streptavidin. The cells were then washed and incubated with Triton X 100 for 10 min at 4°C. The lysed lymphocytes were mixed with 2.6 ml of 2 M-sucrose solution containing 1 mM EDTA, 10 mM HEPES and 1 mM DTT. The lysate was loaded onto a 5 ml sucrose gradient, and the nuclear pellets were obtained by centrifugation at $75,000 \times g$ at 4°C for 60 min. The pellets were carefully removed, washed with PBS, lysed using Triton X100, and centrifuged at $2,000 \times g$. The sedimented fragments were analysed for peptide binding.

CD Spectroscopy (19)—CD measurements were performed on a JASCO J-715 spectropolarimeter. A thin, dry film of artificial liposomes, L-α-phosphatidyl choline (Sigma), was coated on a Quartz cell. Poly [LE] fibrils were layered on the phospholipid monolayer and dried in laminar airflow. Lipid bound Poly [LE] fibrils were scanned at least eight times at the rate of 100 nm/min and the data were averaged. Similarly, a lipid-free poly [LE] dry film alone was scanned to analyze the stability

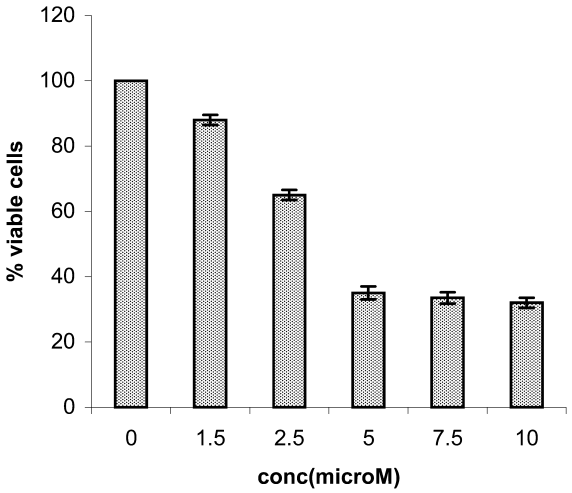

Fig. 1. **Cytotoxic effects of Poly [LE] on lymphocytes as assessed by MTT reduction assay.** Cells were treated with1.5, 2.5, 5,7.5, and 10 μM of Poly [LE].

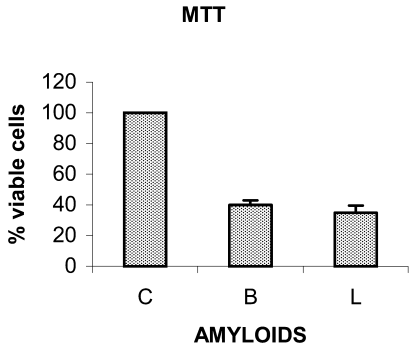

Fig. 2. **Cytotoxic effects of Poly [LE] and Beta amyloid on lymphocytes as assessed by MTT reduction assay.** Cells were treated with 5 μm of PolyLE and Aβ. C, control; B, beta amyloid; L, Poly [LE].

of the beta sheet. The fractional percentages of CD secondary structure were calculated by K_2D prediction.

Statistical Analysis—Data are the averages of triplicates and are expressed as means ± SEM; differences were evaluated by Student's '*t*' test.

RESULTS AND DISCUSSION

The conversion of MTT to colored formazan by mitochondrial reductase serves as an indirect measurement of cellular proliferation and viability. The data in Fig. 1 show the dose dependence of the toxicity of poly [LE] fibrils. The toxicity of poly [LE] depends on dose upto 5 μM, and remains constant at higher concentrations. Figure 2 shows the comparative inhibitory activities of 5 μM Poly [LE] and Aβ25–35 fibrils on the formation of formazan in PBLs. About 35% of Poly [LE] fibril-treated cells remained viable while the viability of the Aβ25–35 treated cells was about 40%. This indicates that Poly (LE) fibrils are more toxic than Aβ25–35 fibrils. The toxicity of amyloids mostly corrrelates with their hydrophobicities and their ability to form amyloid fibrils, their interaction with membranes and the formation of cation selective channels in cellular membranes, together with the activation of voltage dependent calcium channels (*20*). The formation of these channels has been shown to result in ion homeostasis malfunctions and disregulation of cellular signal transduction (*21*), which may lead to cell death. The UV CD spectra were used to determine the effects of phospholipids on the secondary structure of Poly [LE] fibrils. Figure 3 shows the CD spectrum of membrane free and membrane-bound Poly [LE]. This analysis shows that lipid-free Poly [LE] fibrils consist of 43% beta sheet, 9% alpha helix and 48% random coil. The spectrum of the lipid- bound Poly [LE] fibrils shows the presence of 50% beta sheet, 4% alpha helix and 46% random coil. *In vitro* membrane interaction studies reveal that Poly [LE] fibrils interact with phospholipids and their beta sheet structure becomes stabilized in membrane environment. Earlier reports suggest that amyloids interact strongly with phospholipid membranes, and orientate themselves in beta sheet across the surface

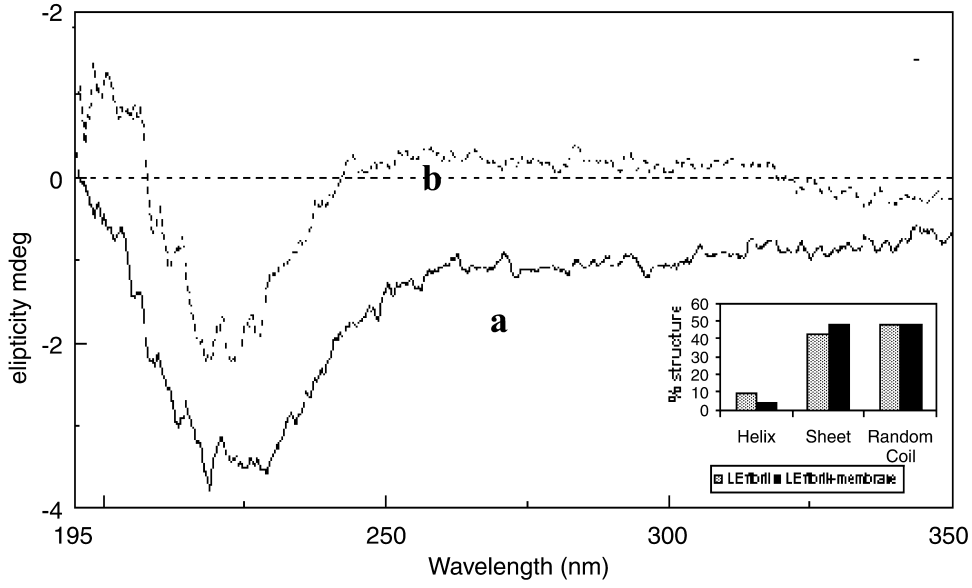

Fig. 3. **CD spectra of Poly [LE] in membrane environment.** a, b represents the interaction of Poly[LE] with and without phosphatidyl choline. Inset plot shows the % change of secondary structure in membrane and non-membranous environment.

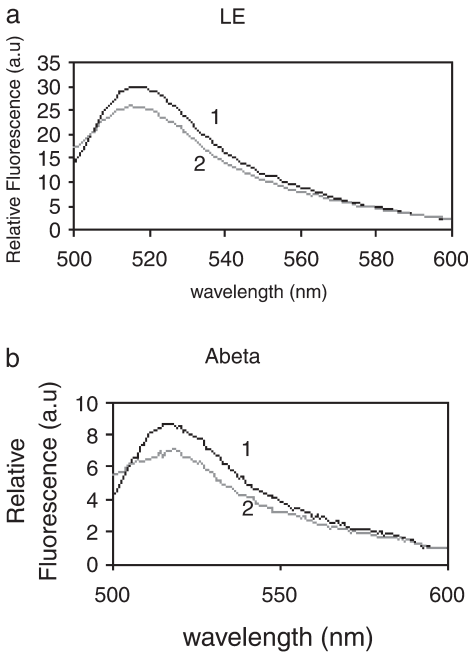

Fig. 4. **Distribution of Poly [LE] and $A\beta_{25-35}$ in Lipid rafts in lymphocyte.** 1 and 2 represent the relative fluorescence of biotinylated amyloids in rafts and non-raft regions. Cells were treated with 5 μm PolyLE and $A\beta_{25-35}$ fibrils.

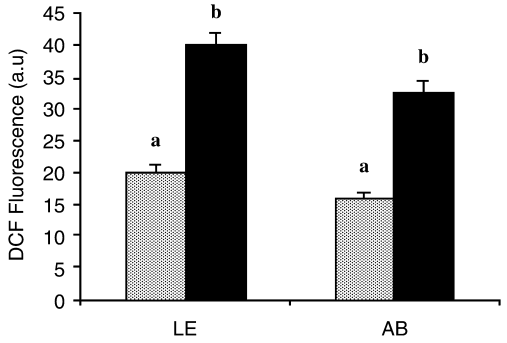

Fig. 5. **Production of reactive oxygen species in amyloid treated lymphocytes as assessed by DCFH-DA fluorescence.** LE and AB indicates the polyLE and beta amyloid treated cells. A and b figure depicts the 5 and 10 μm amyloid concentration, respectively.

of the membrane, with a resulting perturbation of the membrane structure (*22*). Apart from phospholipids, cholesterol plays an important role in the oligomerisation and stabilization of amyloids in a membrane environment. This suggests that lipid rafts may be the vulnerable targets for amyloids and play a role in cellular dysfunction. Studies on lipid raft (Fig. 4, a and b) have revealed that Poly [LE] fibrils have a greater binding affinity for the rafts than Aβ25–35 fibrils. About 55% of the poly [LE] fibrils bind to rafts and 45% to the non-raft regions. In the case of Aβ25–35 fibrils, only 12% bind to the raft region and 10% to non-raft regions. The binding of amyloids to membranes causes significant perturbations and alterations of membrane bound enzymes, especially ATPases, in order to pave the way for entry into cells (*23*). The decrease in total ATPases in cells treated with Poly [LE] fibrils correlates with the above result. The total ATPases activity in cells treated with Poly [LE] fibril is only 10% of that in untreated cells (Table 1a). In Aβ25–35 treated cells, the enzyme activity is about 50%. The impairment of ATPase activity leads to altered ionic homeostasis, which causes a dysregulation of the inflammatory response (*24*). Enhanced inflammatory cytokines activate peroxyl radicals (*25*). Lipid peroxidation was increased by about 30% in cells treated with Poly (LE) fibrils (Table 1b) and those treated with Aβ25–35. High levels of lipid peroxidation lead to the formation of 4-hydroxy-2-noneal (HNE) and acrolein (*26*, *27*). Elevated HNE levels disrupt intracellular organelle calcium homeostasis by oxidizing calcium regulatory proteins, such as the calmodulin (CAM) calcium pumps in mitochondria, and disrupt ATP consumption and stimulates the generation of free radicals, especially superoxide anion. There is an approximate 60% decrease in superoxide dismutase activity in amyloid treated cells (Table 1c), a result that clearly explains the enhanced level of superoxide radicals in the cells. Enhanced DCF fluorescence also confirmed the generation of free radicals in amyloid- treated cells (Fig. 5). GSH is a major intracellular antioxidant with multiple biological functions. One of its most important functions is to protect against oxidative damage caused by ROS generated through enzymatic and nonenzymatic reactions. Impaired intracellular GSH leads to an imbalance in the antioxidant system, and to the generation of free radicals. Intracellular GSH activity decreased by about 40% in Poly [LE] fibril treated cells (Table 1d) and 15% in Aβ25–35 treated cells. The gross decrease in GSH activity in LE treated cells directly correlates with the increase in free radical generation in the cells. The increase in ROS formation leads to the depletion of GSH and to the impairment of the antioxidant system, which, in turn, exacerbates the oxidative damage in amyloid exposed cells (*28*). Peroxynitrile radicals formed by superoxide anions disrupt and oxidize proteins. Protein oxidation regulates the antioxidant enzymes and leads to the aggregation of enzymes (*29*). Drastic decreases in

Table 1. **Percentage decrease in total ATPases, superoxide dismutase, GSH and percentage increase of lipid peroxidation in amyloid treated cells.**

S. No.	Biochemical parameter	Control (%)	LE (%)	$A\beta_{25-35}$ (%)
a	Total ATPases	100	10 ± 3.2	50 ± 2.8
b	Lipid peroxidation	10 ± 1.2	50 ± 2.9	50 ± 3.8
c	Superoxide dismutase	100	40 ± 1.7	40 ± 4.2
d	GSH	100	60 ± 2.8	86 ± 3.2

Lymphocytes were treated with 5 μM of poly [LE] and $A\beta_{25-35}$.Effect of LE and $A\beta_{25-35}$ fibrils on total ATPases, superoxide dismutase, GSH and lipid peroxidation in lymphocytes.

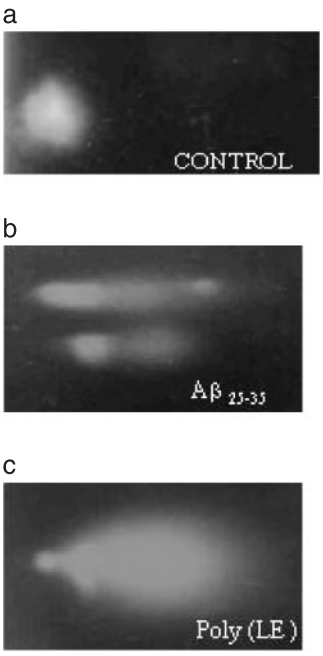

Fig. 6. **Extent of genotoxic effects of amyloids as assessed by Comet assay.** Cells were treated with 5 μm poly [LE] and Beta amyloid. a, control; b, $A\beta_{25-35}$ treated cells; c, Poly[LE] treated cells.

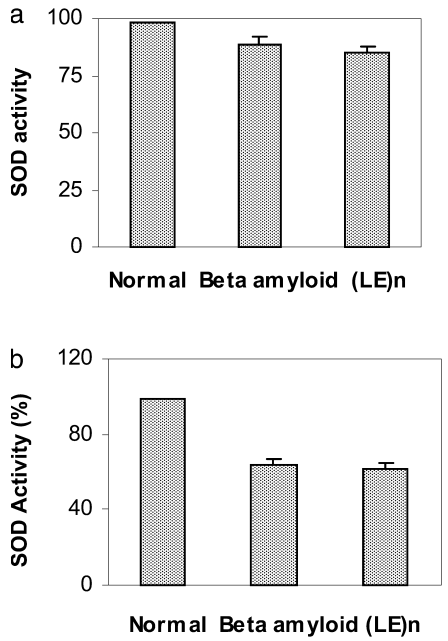

Fig. 8. ***In vitro* inactivation assay of superoxide dismutase by poly [LE] and $A\beta_{25-35}$ at 37°C and 60°C.**

superoxide dismutase activity correlate with the above data. Increased levels of free radicals and decreased activity of superoxide dismutase (only the enzyme actively transported in to nuclei) (*30*) induces genomic damage. The comet assay (Fig. 6) revealed that damage to the nucleus is more pronounced in LE treated cells than in Aβ25–35 treated cells. DNA damage is caused by two major mechanisms, free radical reactions and direct binding to DNA (31). This suggests that apart from oxidative stress to the nucleus, amyloids might bind to the nucleus, thus enhancing their toxic affect. Studies of nuclear membrane interactions studies revealed that poly [LE] binds to the nuclear membrane, but the binding affinity of Aβ25–35 is slightly more pronounced than that of (Fig. 7) poly [LE]. Decreased superoxide activity, a comet like appearance in the comet assay, suggests a gross decrease in superoxide dismutase activity. Apart from the oxidation of these enzymes, amyloids, might bind directly to superoxide dismutase and inhibit its activity. *In vitro* assays of superoxide dismutase activity reveal that poly [LE]-incubated solutions lose about 15% of their activity at room temperature compared to about 12% for Aβ25–35 treated solutions (Fig. 8a). Superoxide dismutase loses about 40% of its activity when preheated with poly [LE] at 60°C, compared with 37% for the Aβ25–35 treated enzyme (Fig. 8b). This shows that under physiological conditions and slightly perturbed conditions involving mild stress, amyloids might bind to enzymes causing aggregation and preventing them from retaining their native structures.

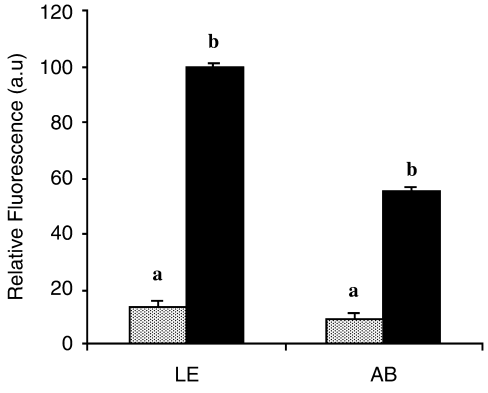

Fig. 7. **Binding of amyloids to nuclear membranes in lymphocytes.** LE and AB indicate the biotinylated polyLE and $A\beta_{25-35}$ treated cells. a and b figure indicate the 5 and 10 μM concentrations, respectively.

This study suggests that Poly [LE] can act, as an ideal peptide to mimic amyloids, and that toxicity of Poly [LE] is due to the potent induction of beta sheet structures promoted by interactions with negative membrane surfaces. This study also reveals that membranes may act as conformational catalysts or chaperones for amyloids.

We are grateful to Dr. T. Ramasami, Director, CLRI, Chennai for his kind permission to publish this work. We are thankful to Dr. S. Niranjali Devaraj for revising the manuscript. We also thank Ms. Julia P. Moses for her support. J. M and D.K. acknowledge the CSIR for financial support in the form of Senior Research Fellowships.

REFERENCES

1. Temossi, D.A., Masino, L., and Pastoro, A. (2003) From Alzhemier's to Huntington: why is a structural understanding so difficult? *EMBO J.* **22**, 355–361
2. Murphy, R.M. (2002) Peptide aggregation in neurodegenerative disease. *Annu. Rev. Biomed. Eng.* **4**, 155–174

3. McGowan, D.P., Van Roon-mom, W., Holloway, H., Bates, G.P., and Mangiariani, L. (2000) Amyloid-like inclusions in Huntington's disease. *Neuroscience* **100**, 677–680
4. Soto, C., Castano, E.M., Kumar, R.A., Beavis, R.C., and Frangione, B. (1995) Fibrillogenesis of synthetic amyloid-beta peptides is dependent on their initial secondary structure. *Neurosci. Lett.* **200**, 105–108
5. Janek, K., Behlke, J., Zipper, J., Fabian, H., Georgalis, Y., Beyermann, M., Bienert, M., and Krause, E. (1999) Water-soluble beta-sheet models which self-assemble into fibrillar structures. *Biochemistry* **29**, 8246–8252
6. Hatters, D.M., MacRaild, C.A., Daniels, R., Gosal, W.S., Thomson, N.H., Jones, J.A., Davis, J.J., MacPhee, C.E., Dobson, C.M., and Howlett, G.J. (2003) The circularization of amyloid fibrils formed by apolipoprotein C-II. *Biophys. J.* **85**, 3979–3990
7. Julia, P., Moses, Satheeshkumar, K.S., Murali, J., Alli, D., and Jayakumar, R. (2003) Self-assembly of the Ssynthetic polymer (Leu-Glu)n: An amyloid-like structure formation. *Langmuir* **19**, 3413–3418
8. Mecocci, P., Polidori, M.C., Cherubini, A., Ingegni, T., Mattioli, P., Catani, M., Rinaldi, P., Cecchetti, R., Stahl, W., Senin, U., and Beal, M.F. (2002) Lymphocyte oxidative DNA damage and plasma antioxidants in Alzheimer disease. *Arch. Neurol.* **59**, 794–798
9. Ranthell, J.C. and Thompson, C.B. (1999) The cental effectors of cell death in the immune system. *Annu. Rev. Immunol.* **17**, 781–828
10. Liu, K.Z., Schultz, C.P., Johnston, J.B., Lee, K., and Mantsch, H.H. (1997) Comparison of infrared spectra of CLL cells with their ex vivo sensitivity (MTT assay) to chlorambucil and cladribine. *Leuk. Res.* **21**, 1125–1133
11. Ohkawa, H., Ohishi, N., and Yagi, K. (1978) Reaction of linoleic acid hydroperoxide with thiobarbituric acid. *J. Lipid. Res.* **19**, 1053–1057
12. Moron, M.S., Depierre, J.M., and Maunervik, B. (1979) Levels of glutathione, glutathione reductase and glutathione S-transferase activities in rat lung and liver. *Biochim. Biophys. Acta* **582**, 67–78
13. Misra, H.P. and Fridovich, I. (1972) The role of superoxide anion in the autoxidation of epinephrine and a simple assay for superoxide dismutase. *J. Biol. Chem.* **247**, 3170–3175
14. Evans, W.H. (1978) In *Preparation and Characterization of Mammalian Plasma Membrane—Part I*, pp. 177–183, Elsevier/North Holland Biomedical, Amsterdam
15. Speit, G. and Bonzheim, I. (2003) Genotoxic and protective effects of hyperbaric oxygen in A549 lung cells. *Mutagenesis* **18**, 545–548
16. Nakamura, K., Fushimi, K., Kouchi, H., Mihara, K., Miyazaki, M., Ohe, T., and Namba, M. (1998) Inhibitory effects of antioxidants on neonatal rat cardiac myocyte hypertrophy induced by tumor necrosis factor-alpha and angiotensin II. *Circulation* **98**, 794–799
17. Brown , D.A. and London, E.(2000) Structure and function of sphingolipid- and cholesterol-rich membrane rafts. *J. Biol. Chem.* **275**, 17221–17224
18. Blomqvist, M., Bergquist, J., Westman, A., Kansson, K.H., kansson, P.H., Fredman, P., and Ekman, R. (1999) Identification of defensins in human lymphocyte nuclei. *Eur. J. Biochem.* **263**, 312–318
19. Rymer, D.L. and Good, T.A. (2000) The role of prion peptide structure and aggregation in toxicity and membrane binding. *J. Neurochem.* **75**, 2536–2545
20. Mark, R.J., Hensley, K., Butterfield, D.A., and Mattson, M.P. (1995) Amyloid beta-peptide impairs ion-motive ATPase activities: evidence for a role in loss of neuronal Ca^{2+} homeostasis and cell death. *Neuroscience* **15**, 6239–6249
21. Lahdo, R., Coillet-Matillon, S., Chauvet, J.P., and de La Fourniere-Bessueille, L. (2002) The amyloid precursor protein interacts with neutral lipids. *Eur. J. Biochem.* **269**, 2238–2246
22. Gibson Wood, W., Eckert, G.P., Igbavboa, U., and Muller, W.E. (2003) Amyloid beta-protein interactions with membranes and cholesterol: causes or casualties of Alzheimer's disease. *Biochim. Biophys. Acta* **1610**, 281–290
23. Xiao, A.Y., Wang, X.Q., Yang, A., and Yu, S.P. (2002). Slight impairment of Na^+, K^+-ATPase synergistically aggravates ceramide- and beta-amyloid-induced apoptosis in cortical neurons. *Brain Res.* **955**, 253–259
24. Chun, C.C., Shuxian, H., and Phillip, K.P. (1998) *Alzheimer's Disease Review* **3**, 87–90
25. Butterfield, A. and Lauderback, C.M. (2002). Lipid peroxidation and protein oxidation in Alzheimer's disease brain: potential causes and consequences involving amyloid beta-peptide-associated free radical oxidative stress. *Free Radic. Biol. Med.* **32**, 1050–1060
26. Mattson, M.P. and Chan, S.L. (2003) Neuronal and glial calcium signaling in Alzheimer's disease. *Cell Calcium* **34**, 385–397
27. Butterfield, D., Hensley, K., Harris, M., Mattson, M., and Carney, J. (1994) Beta-Amyloid peptide free radical fragments initiate synaptosomal lipoperoxidation in a sequence-specific fashion: implications to Alzheimer's disease. *Biochem. Biophys. Res. Commun.* **200**, 710–715
28. Pocernich, C.B., Cardin, A.L., Racine, C.L., Lauderback, C.L., and Butterfield, D.A. (2001) Glutathione elevation and its protective role in acrolein-induced protein damage in synaptosomal membranes: relevance to brain lipid peroxidation in neurodegenerative disease. *Neurochem. Int.* **39**, 141–149
29. Butterfield, A. and Kanski, J. (2001) Brain protein oxidation in age-related neurodegenerative disorders that are associated with aggregated proteins. *Mech. Ageing Dev.* **122**, 945–962
30. Ookawara, T., Eguchi, H., Nishimura, M., Kizaki, T., Takayama, E., Saitoh, D., Ohno, H., and Suzuki, K. (2003) Effects of oxidative stress on the nuclear translocation of extracellular superoxide dismutase. *Biochem. Biophys. Res. Commun.* **303**, 914–919
40. Santiard-Baron, D., Lacoste, A., Ellouk-Achard, S., Soulie, C., Nicole, A., Sarasin, A., and Ceballos-Picot, I. (2001) The amyloid peptide induces early genotoxic damage in human preneuron NT2. *Mutat. Res.* **479**, 113–120